Electroluminescence yield in xenon gas detectors

C.M.B. Monteiro[1,*], L.M.P. Fernandes[1], J.A.M. Lopes[1,2], L.C.C. Coelho[1], J.F.C.A. Veloso[3], J.M.F. dos Santos[1], K. Giboni[4], E. Aprile[4]

[1]GIAN, Physics Department, University of Coimbra, 3004-516 Coimbra, Portugal

[2]Instituto Superior de Engenharia de Coimbra, Apartado 4065, 3030-199 Coimbra, Portugal

[3]Physics Department, University of Aveiro, 3810-193 Aveiro, Portugal

[4]Physics Department and Columbia Astrophysics Laboratory, Columbia University, New York, New York 10027, USA

*Corresponding author: cristina@gian.fis.uc.pt

Abstract – **The electroluminescence yield was studied for xenon gas as a function of the electric field in the scintillation region, for room temperature using a gas proportional scintillation counter. A large area avalanche photodiode was used for the readout of the VUV secondary scintillation produced in the gas, together with the 5.9-keV x-rays directly absorbed in the photodiode. Using the latter as a reference for the number of charge carriers produced by the scintillation pulse, it was possible to determine the number of VUV photons impinging the photodiode. This way, a scintillation amplification parameter of 140 photons/kV was obtained. The attained results are in good agreement with those predicted, for room temperature, by Monte Carlo simulation and Boltzmann calculations, as well as with those obtained for saturated xenon vapour, at cryogenic temperatures, and are about a factor of two higher than former results measured at room temperature.**

I. INTRODUCTION

Xenon gas counters have been widely used as x-ray and low-energy γ-ray detectors [1]. Since long, gas detectors have been used intensively in nuclear medicine and medical imaging [2,3]. In both cases, signal amplification in the gas is achieved by accelerating the electrons resulting from the radiation interaction to excite the gas atoms by electron impact, leading to the production of secondary scintillation, the so-called electroluminescence, defined as the number of secondary scintillation photons produced per drifting electron per unit path length.

These electrons are lead to the scintillation region, where they can acquire enough energy from the electric field to excite the noble gas atoms through inelastic collisions. Between two successive inelastic collisions, the electrons undergo a very large number of elastic collisions, above 10^4 [4], while they gain enough energy from the electric field to excite the atoms. Nevertheless, the amount of energy lost in these elastic collisions is small, given the large mass difference between electron and Xe atom. The excitation efficiency, i.e. the fraction of energy acquired from the electric field by the electron that is spent in exciting the xenon atoms, reaches values of ~95% for values of *E/p* (the electric field divided by the gas pressure) of 4 kV cm^{-1} bar^{-1} [4,5]. This energy loss, however, is not negligible for low values of *E/p*, as the number of elastic collisions increases significantly. The excitation efficiency presents a fast decrease for values of *E/p* below 2 kV cm^{-1} bar^{-1} [4,5], being zero below a characteristic *E/p* threshold, below which electrons never acquire enough energy to excite the gas atoms.

The mechanisms of secondary scintillation production are well known [4,6-8]. For pure xenon, the wavelength of the emission depends on the gas pressure and, above 400 mbar, the secondary scintillation presents a narrow peak, ~10 nm FWHM, centred at 172 nm [7]. The overall scintillation efficiency reaches values of 80% for *E/p* of 4 kV cm^{-1} bar^{-1} [4,5].

The data for electroluminescence in the literature yield are not in agreement. While those obtained for room temperature using Monte Carlo simulation [5] and Boltzman calculations [9] agree perfectly, the values obtained experimentally [10-15] are much lower than the former and differ significantly from each other. On the other hand, the results presented for saturated gas at cryogenic temperatures [14,15], in equilibrium with the liquid phase, are in agreement with each other, as well as with the simulation results calculated for room temperature.

Absolute measurements are difficult to perform and usually rely on comparison/calibration performed with experimental set-ups and/or settings other than those used to measure the secondary scintillation in itself, e.g. Ref. [15].

In this work, we apply a straightforward method, using only one experimental set-up to carry out absolute electroluminescence yield measurements. A VUV-sensitive large area avalanche photodiode (LAAPD) detects, simultaneously, the secondary scintillation of a xenon gas proportional scintillation counter (GPSC) and original x-rays. The latter are used as reference for determining the absolute number of VUV-photons reaching the LAAPD. The electroluminescence yield is measured as a function of electric field in the scintillation region and is compared with the other experimental and calculated results found in the literature.

II. EXPERIMENTAL SETUP

A xenon-filled GPSC instrumented with a large area APD

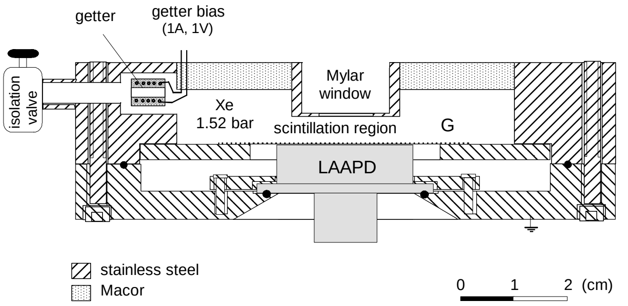

Fig. 1 - Schematic of the driftless GPSC used in the present work.

was used. The driftless GPSC is schematically depicted in Fig. 1 and was already used in Refs. [16,17]. The detector is pumped down to pressures in the 10^{-6} mbar range, and filled with high purity xenon at a pressure of 1.52 bar. The gas purity in the detector is maintained by a small non-evaporable getter (SAES ST172/HI/7-6/150C).

For this study, we have used a 1-mm collimated 5.9-keV x-ray beam from a ^{55}Fe x-ray source filtered with a Cr-film to remove the 6.4-keV Mn K_β-fluorescence line. X-rays entering the radiation window are absorbed in the gas by photoelectric effect, generating a primary electron cloud. The electrons are accelerated in the electric field. Each primary electron produces a large number of VUV photons. Proportionality between incident x-ray energy, number of primary electrons and number of scintillation photons is maintained throughout the process.

The electron–hole pairs produced in the sensitive area of the APD by absorption of the scintillation photons are multiplied by the avalanche process. Concurrent with the acquisition of the scintillation signals resulting from the absorption of x-rays in xenon, a transmitted fraction of the x-rays is detected directly by the APD. The number of electron–hole pairs produced through direct absorption of the x-rays in the APD is determined from the energy of the x-ray and the *w*-value in silicon, i.e. the mean energy required to produce a pair of charge carriers. The APD reverse bias voltage determines the multiplication gain in the avalanche process.

For each 5.9-keV x-ray interaction in the driftless detector, the total number of scintillation photons produced by the primary electron cloud will depend on how deep into the scintillation region the x-ray is absorbed. Nevertheless, the average number of VUV photons is well defined, as the respective pulse-height distribution has a Gaussian shape with a tail towards the low energy region. Although the driftless GPSC results in degraded energy resolution for scintillation events, it allows a higher transmission of the 5.9-keV x-rays through xenon and, therefore, more direct x-ray interactions in the APD, convenient for this study. In our case, approximately 0.2% of the 5.9-keV x-rays are transmitted through 1.1 cm of xenon.

The charge pulses collected in the APD are integrated in a 1.5 VpC^{-1} charge-sensitive preamplifier (Canberra 2004), followed by linear amplification (Hewlett Packard 5582A) with a 2-μs shaping time. Pulse-height analysis is performed with a 1024-channel analyser (Nucleus PCA-II). The peaks in the pulse-height distribution are fit to a Gaussian function superimposed on a linear background.

III. METHOD

Figure 2 depicts a typical pulse height distribution obtained with the driftless GPSC instrumented with an LAAPD for scintillation readout.

The salient features of the pulse-height distribution include, not only the 5.9-keV x-ray full-energy peak from absorption in the xenon GPSC, but also the xenon L_α- and L_β-escape peaks from 5.9-keV x-ray absorption in the xenon GPSC, the 5.9-keV x-ray peak from direct absorption in the APD, the 4.1- and 4.8-keV xenon L_α- and L_β-fluorescence peaks from absorption in the APD, and the system electronic noise. The pulse-height distributions enable a direct comparison between the pulse amplitudes resulting from the 5.9-keV x-ray full-absorption in the gas, i.e. from the xenon scintillation, and direct absorption in the APD. This allows a direct quantification of the VUV-photons impinging the LAAPD, given the quantum efficiency of the device.

A value of QE = 1.1 for the number of charge carriers

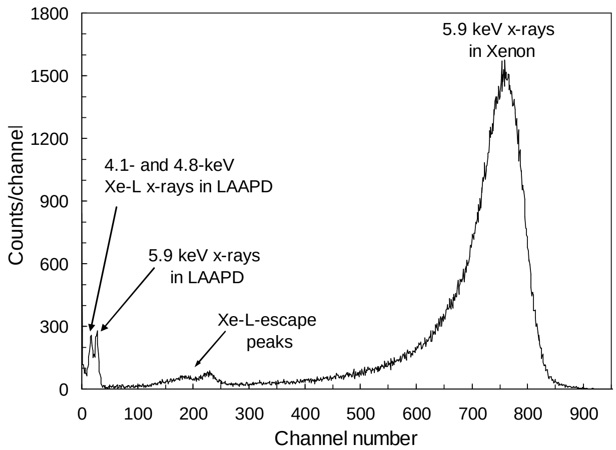

Fig. 2 - Pulse-height distribution from a xenon driftless GPSC instrumented with a large-area APD, for 5.9-keV X-rays. An *E/p* of 4.1 kVcm^{-1}bar^{-1} was used in the scintillation region.

produced in the photodiode per incident 172-nm VUV photon was provided by the manufacturer [18] for the LAAPDs we acquired [19]. We assume an uncertainty of ~ 0.1 for the LAAPD quantum efficiency. This uncertainty is the major source of error in our measurements.

For a reduced electric field of 4.1 kVcm^{-1}bar^{-1}, the ratio between the pulse amplitudes resulting from the 5.9-keV x-ray full-absorption in the gas and absorbed in the APD, as obtained from the corresponding pulse-height distribution, is 19.9±0.1 for low LAAPD gains, where gain non-linearity in the photodiode is less than 1% [16]. As the *w*-value in silicon is 3.62 eV [20], in xenon is 22.4 eV [22], the average solid angle subtended by the photosensor active area for the primary electron path, computed through Monte Carlo [21], delivered a value of ≅ 0.202 for the present geometry, the average distance the primary electron cloud drifts in the detector is 0.93 cm, the reduced scintillation yield, *Y/p*, determined for 4.1 $kVcm^{-1}bar^{-1}$ is 466 photons per electron per cm of path and per bar.

IV. EXPERIMENTAL RESULTS AND DISCUSSION

Table I summarizes the different values found in the literature for the scintillation amplification parameter, and the respective experimental conditions concerning pressure and temperature. Our results are in good agreement with those obtained by Monte Carlo and Boltzmann simulations for room temperature.

The scintillation amplification parameter - the number of photons produced per drifting electron and per volt, represented by the slope of the linear dependence - presents many different values in the literature and is not well established yet. Above a reduced field of 8 $kVcm^{-1}bar^{-1}$, the xenon ionisation threshold, the reduced scintillation yield variation departs from the linear behaviour, reflecting the exponential growth in the number of electrons in the scintillation region, since secondary electrons also produce electroluminescence, while *Y/N* is calculated per primary electron. Favata et al. [23] compiled the different studies on electroluminescence yield published up to then (1990), concluding that the reduced electroluminescence yield is pressure-independent. Fonseca et al. [15] have shown that the scintillation yield does not depend on gas temperature, in the range from 20 downto -88ºC. On the other hand, for -90ºC and at a constant gas pressure, the scintillation amplification factor near the saturation point varies significantly, depending on the amount of xenon present in the liquid phase.

The value of 70 photons/kV, obtained by Parsons et al. (1989) [11] and confirmed by Bolozdynya et al. (1997) [12] and Akimov et al. (1997) [13] is a factor of two lower than that obtained by Monte Carlo simulation and Boltzmann calculation. In 2003, Aprile et al. [14] estimated a value of 120 photons/kV in saturated xenon vapour, in much better agreement with the simulation. The value obtained by Fonseca et al. [15] in saturated xenon vapour, at -90ºC, is in very good agreement with that obtained by simulation for room temperature, but their value obtained at room temperature is only ~90 photons/kV, similar to Ngoc et al. (1980) [10].

Our measurements show for the first time that, even for room temperature, the scintillation amplification parameter can be as high as those predicted by Monte Carlo simulation and/or Boltzmann analysis and those experimentally obtained for saturated xenon vapour at cryogenic temperatures. We attribute the differences in the experimental values obtained at room temperature to different levels of gas purity achieved in each experimental set-up: higher impurity content will result in less efficient energy transfer from electric field to photons, leading to lower scintillation amplification values.

V. CONCLUSION

The reduced electroluminescence yield of pure xenon at room temperature was studied and compared with other results in the literature. The measurements were performed with a gas proportional scintillation counter (GPSC) instrumented with a LAAPD for the VUV secondary scintillation readout. X-rays with energy of 5.9 keV were used to induce the secondary scintillation in the GPSC or partially to interact in the photodiode. The direct interactions are used as a reference for the determination of the number of charge carriers produced by the scintillation pulse and, thus, the number of VUV photons impinging the photodiode, given its quantum efficiency.

A scintillation amplification parameter, i.e., number of photons produced per drifting electron and per volt, of 140 photons/kV, was measured. The results are in good

Work	Amplification parameter (photons/kV)	linear trend		Pressure	Temperature
		Density units*	Pressure units**		
Present work	140	*Y/N* = 0.140 *E/N* -0.474	*Y/p* = 140 *E/p* -116	1.52 bar	20ºC
Santos et al. (MC) [7]	139	*Y/N* = 0.139 *E/N* -0.402	*Y/p* = 139 *E/p* -100	1 atm	20ºC
Fraga et al. (Boltzmann) [11]	138	*Y/N* = 0.138 *E/N* -0.413	*Y/p* = 138 *E/p* -102	1 atm	20ºC
Fonseca et al. [17]	137	*Y/N* = 0.137 *E/N* -0.470	*Y/p* = 137 *E/p* -125	2 bar	-90ºC
Aprile et al. [16]	120	*Y/N* = 0.120 *E/N* -0.378	*Y/p* = 120 *E/p* -154	2 atm	-95ºC
Ngoc et al. [12]	88	*Y/N* = 0.088 *E/N* -0.479	*Y/p* = 88 *E/p* -113	2 - 10 atm	20ºC
Fonseca et al. [17]	86	*Y/N* = 0.086 *E/N* -0.296	*Y/p* = 86 *E/p* -73	2 bar	20ºC
Parsons et al. [13]	70	*Y/N* = 0.070 *E/N* -0.255	*Y/p* = 70 *E/p* -63	5 atm	20ºC
Bolozdynya et al. [14]	70	*Y/N* = 0.070 *E/N* -0.283	*Y/p* = 70 *E/p* -70	-	20ºC
Akimov et al. [15]	70	*Y/N* = 0.070 *E/N* -0.224	*Y/p* = 70 *E/p* -56	2, 4, 8 atm	20ºC

* *E/N* in Td (10^{-17} V cm^2 $atom^{-1}$)

** *E/p* in kV cm^{-1} bar^{-1}

Table. 1 - Xenon secondary scintillation amplification parameter, reduced electroluminescence yield linear trends and experimental conditions of pressure and temperature for this work, as well as for the different data reported in the literature agreement with those predicted by Monte Carlo simulation and Boltzmann calculation for room temperature and also with those observed for saturated xenon vapour at cryogenic temperatures. Our result is about a factor of two higher than earlier results measured at room temperature. Differences in gas purity during the experimental measurements may be one of the factors responsible for the different experimental results obtained at room temperature.

VI. ACKNOWLEDGEMENTS

Support is acknowledged from project POCI/FIS/60534/2004 through FEDER and FCT (Lisbon). C.M.B. Monteiro acknowledges grant BD/35569/2005 from FCT.

REFERENCES

[1] J.M.F. Dos Santos et al., “Development of portable gas proportional scintillation counters for x-ray spectrometry”, X-Ray Spectrom. **30** (2001) 373.

[2] A. Barr et al., “A high-speed, pressurised multi-wire gamma camera for dynamic imaging in nuclear medicine”, Nucl. Instrum. Meth. A **477** (2002) 499.

[3] C. Grignon *et al*. “Simulation of a high performance γ-camera concept for PET based on liquid xenon and gaseous photomultiplier”, 2005 IEEE International Conference on Dielectric Liquids (2005) 357.

[4] T.H.V.T. Dias et al., “Monte Carlo simulation of x-ray absorption and electron drift in gaseous xenon”, Phys. Rev. A **48** (1993) 2887.

[5] F.P. Santos et al., “Three dimensional Monte Carlo calculation of the VUV electroluminescence and other electron transport parameters in xenon”, J. Phys. D: Appl. Phys. **27** (1994) 42.

[6] M. Suzuki, S. Kubota, “Mechanism of proportional scintillation in argon, krypton and xenon”, Nucl. Instrum. Meth. 164 (1979) 197.

[7] M.S.C.P. Leite, “Radioluminescence of rare gases”, Portugal. Phys. **11** (1980) 53.

[8] T. Takahashi et al., “Emission spectra from Ar-Xe, Ar-Kr, Ar-N2, Ar-CH4, Ar-CO2 and Xe-N2 gas scintillation proportional counters”, Nucl. Instrum. Meth. **205** (1983) 591.

[9] M.M.F.R. Fraga et al., presented at the 1990 ESCAMPIG, 28-31 Aug., Orleans, France.

[10] H.N. Ngoc et al., “A xenon high-pressure proportional scintillation camera for x and γ-ray imaging”, Nucl. Instrum. Meth. **172** (1980) 603.

[11] A. Parsons et al., “High pressure gas scintillation drift chambers with wave shifter fiber readout”, IEEE Trans. Nucl. Sci. **36** (1989) 931.

[12] A. Bolozdynya et al., “A high-pressure xenon self-triggered scintillation drift chamber with 3D sensitivity in the range of 20-140 keV deposited energy”, Nucl. Instrum. Meth. A **385** (1997) 225.

[13] D.Y. Akimov et al., “Development of high pressure Xe scintillation proportional counter for experiments in “low-background” physics”, arXiv:hep-ex/9703011 v1 20 Mar 1997.

[14] E. Aprile et al., “Proportional Light in a Dual-Phase Xenon Chamber”, IEEE Trans. Nucl. Sci. **51** (2004) 1986; presented at the IEEE Nucl. Sci. Symp., November 2003, Seattle, USA.

[15] A.C. Fonseca et al., “Study of Secondary Scintillation in Xenon Vapour”, *2004 IEEE Nucl. Sci. Symp. Conference Record (2005).*

[16] L.M.P. Fernandes et al., “Non-linear behavior of large-area avalanche photodiodes”, Nucl. Instrum. Meth. A **478** (2002) 395.

[17] J.F.C.Veloso et al., “Gas proportional scintillation counters for the μp Lamb-shift experiment”, IEEE Trans. Nucl. Sci. **49** (2002) 899.

[18] B. Zhou, M. Szawlowski, “An explanation on the APD spectral quantum efficiency in the deep UV range”, Interoffice Memo, Advanced Photonix Inc., 1240 Avenida Acaso, Camarillo, CA 93012, EUA, 1999.

[19] J.A.M. Lopes, et al., “A xenon gas proportional scintillation counter with a UV-sensitive, large-area avalanche photodiode”, IEEE Trans. Nucl. Sci., **48** (2001) 312-319.

[20] G.F. Knoll, “Radiation Detection and Measurement”, 3rd Edition, Wiley, New York, 2000.

[21] J.M.F. dos Santos et al., “The dependence of the energy resolution of gas proportional scintillation counters on the scintillation region to photomultiplier distance”, IEEE Trans. Nucl. Sci. **39** (1992) 541.

[22] T.H.V.T. Dias et al., “Full-energy absorption of x-ray energies near the Xe L-and K-photoionization thresholds in xenon gas detectors: Simulation and experimental results”, J. Appl. Phys. **82** (1997) 2742.

[23] F. Favata et al., “Light yield as a function of gas pressure and electric field in gas scintillation proportional counters”, Nucl. Instrum. Meth. A **294** (1990) 595.